Biophysical Chemistry 18 (1983) 153–163
Elsevier

BPC 00791

Ca^{2+}-GRAMICIDIN A INTERACTIONS AND BLOCKING EFFECTS ON THE IONIC CHANNEL

F. HEITZ and C. GAVACH

Laboratoire de Physico-chimie des Système Polyphasés, LA.330, C.N.R.S., Route de Mende, B.P. 5051, 34033 Montpellier Cedex, France

Received 5th January 1983
Revised manuscript received 28th April 1983
Accepted 2nd May 1983

Key words: Gramicidin channel; Ca^{2+} blocking; Ca^{2+}-gramicidin interaction; Single channel

From spectroscopic data (infrared, CD and ^{13}C-NMR) it is shown that Ca^{2+} interacts with gramicidin A and that a head-to-head gramicidin A dimer can have two Ca^{2+}-binding sites located near the COOH termini. On the basis of this result, we can propose an explanation for the blocking effect of Ca^{2+} on the transport of alkali metal ions (Cs^+ and K^+) through gramicidin channels. The binding of Ca^{2+} is competitive with the alkali metal ion binding: Ca^{2+} cannot cross the gramicidin channel and its binding in the channel is voltage dependent. From the proposed model, it is possible to account for the influence of the addition of Ca^{2+} on the single-channel limiting conductance and on the variation of the single-channel current as a function of the voltage in the presence of Cs^+ or K^+.

1. Introduction

In recent years, much attention has been devoted to the study of gramicidin A: HCO-L-Val-Gly-L-Ala-D-Leu-L-Ala-D-Val-L-Val-D-Val-L-Trp-D-Leu-L-Trp-D-Leu-L-Trp-D-Leu-L-Trp-NHC_2H_4-OH [1]. When introduced into a lipid bilayer, this molecule is thought to form a head-to-head dimer of $\pi^6_{L\text{-}D}$ helices [2,3] with an intramolecular channel permeable to monovalent alkali metal ions [4–7]. The gramicidin-induced conductance was shown to be made up of discrete, well defined units [5,6].

However, several questions remain open. Among them, besides the possible role of the side chains [8,9], the blocking effect of the gramicidin channel by divalent cations such as Ca^{2+} or Ba^{2+} is still obscure. It was first suggested by Bamberg and Läuger [10] that these ions bind to a site at or near the channel mouth, thereby reducing the rate at which permeable ions enter and leave the channel. More recently, Urry et al. [11] showed that divalent ions can enter the ion-binding site which is located inside the channel while Eisenman et al. [12] suggest that Ca^{2+} binds at an outer site and therefore lowers the effective concentration of permeant cations in the channel without altering the relative energy barrier heights at the middle versus the mouth.

In order to clarify this problem, we have undertaken the study of interactions between gramicidin and calcium using spectroscopic techniques and tried to relate them with the Ca^{2+} blocking effect on the channel conductance in the presence of Cs^+ and K^+.

2. Experimental section

All the experiments were performed on commercial gramicidin which is a mixture of gramicidin A, B and C (Sigma). It was recrystallized from ethanol before use. All solvents were spectrograde and used without further purification.

Infrared spectra were recorded on a Perkin-Elmer spectrophotometer using 50 μm thick CaF_2

cells. Circular dichroism (CD) experiments were performed on a Roussel-Jouan dicrograph Mark III using 10- and 1-mm thick cells according to the region observed.

^{13}C-NMR spectra were recorded on 150 mg/ml solutions at 35 ± 2°C on a Bruker WH 90 spectrometer working in the Fourier transform mode with proton noise decoupling. The spectrometer was locked on the deuterium resonance of the solvent (C^2H_3OH or $C_2H_5O^2H$) and $(CH_3)_4Si$ was used as internal reference. Addition of calcium was made by dissolution of the chloride salt in the gramicidin solution.

For single-channel experiments, black lipid membranes were formed from a 2% solution of glyceryl monooleate (Sigma) in decane using Teflon cells filled with the aqueous electrolyte solutions. The membrane areas were about $0.3–0.5 \times 10^{-3}$ cm^2. A current-to-voltage converter (Keithley model 427) was used as current amplifier and the current fluctuations were stored on a microcomputer Apple II. Frequency sampling was 50 Hz. gramicidin was added from a solution in ethanol to the aqueous phases. When the aqueous sides of a membrane were different, the electrode potential of each electrode was measured by means of a Keithly 619 electrometer/multimeter using a calomel electrode as reference.

3. Results

3.1. Spectroscopic investigations

3.1.1. Infrared spectroscopy

In ethanol, when the calcium/gramicidin ratio (R) is increased up to 10, the infrared spectrum shows drastic modifications in the amide I region (fig. 1). Indeed, the amide I band is shifted from 1637 cm^{-1} for $R = 0$ to 1653 cm^{-1} for $R = 10$, suggesting that gramicidin A undergoes a calcium-induced transconformation. Further, as shown in fig. 2, this transconformation is not instantaneous.

When gramicidin is dissolved in methanol, a similar behavior is observed up to $R = 2$, i.e., a decrease of the amide I band located at 1637 cm^{-1} accompanied by an increase of that at 1653 cm^{-1}

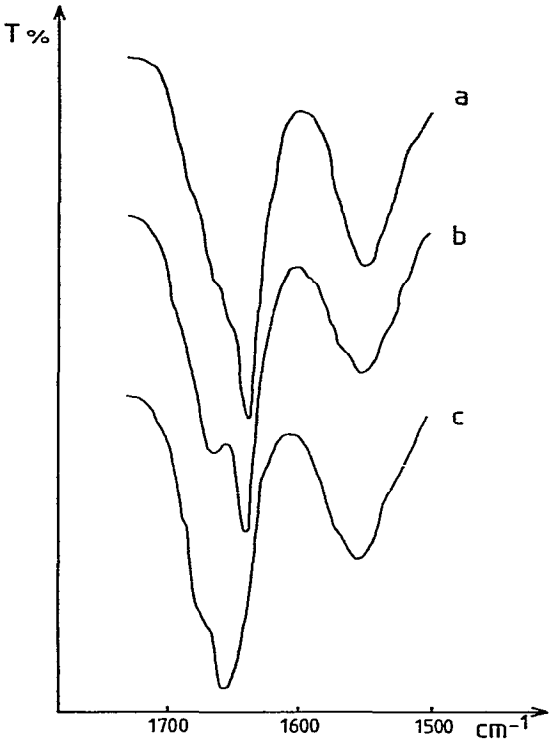

Fig. 1. Infrared spectra in ethanol for various calcium/gramicidin A (R) ratios. (a) $R = 0$. (b) $R = 1$. (c) $R = 10$.

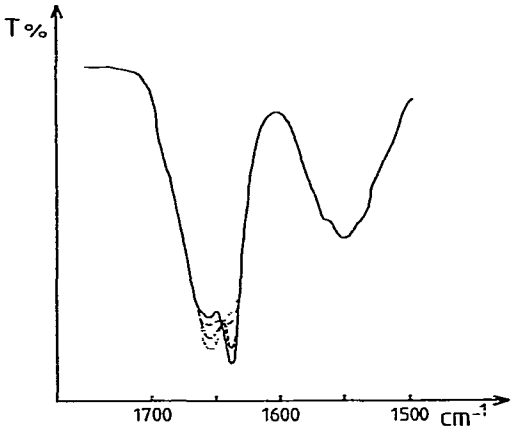

Fig. 2. Kinetic effect at $R = 5$ on the calcium-induced transconformation of gramicidin A. The spectra were recorded 2 (———), 7 (- - - - - -), 12 (·—·—·) and 22 (· · · · · ·) min after addition of $CaCl_2$ to the gramicidin solution.

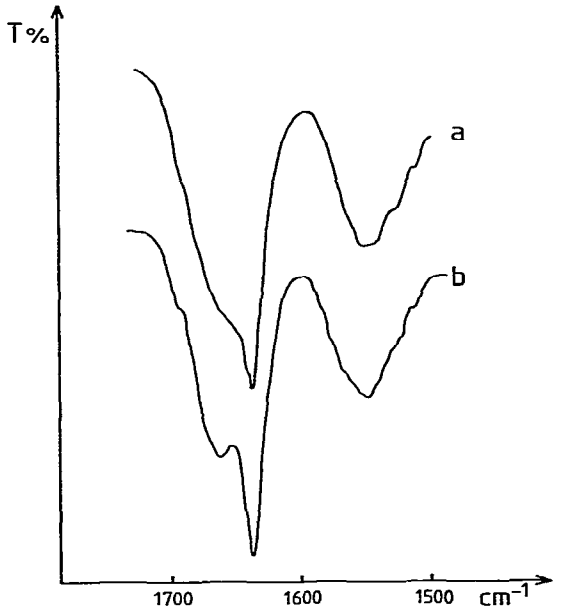

Fig. 3. Infrared spectra in methanol for various calcium/gramicidin ratios. (a) $R = 0$. (b) $R = 2$.

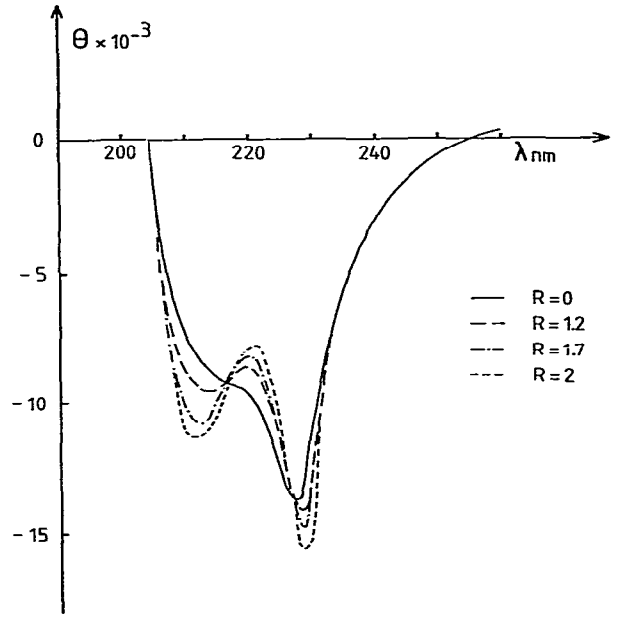

Fig. 4. CD spectra (peptide region) in ethanol for various values of R. θ is the residue ellipticity.

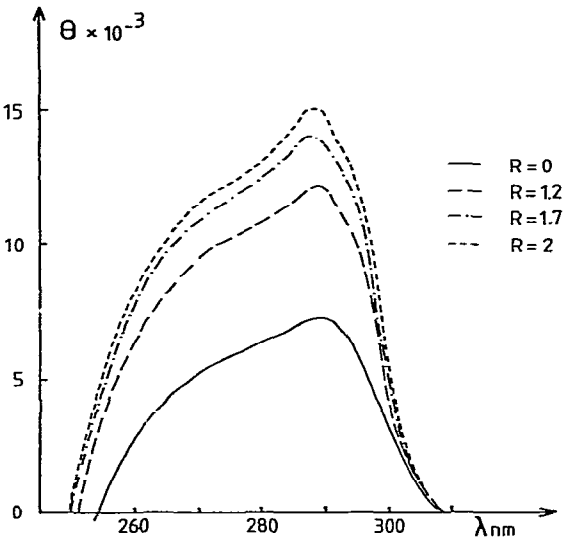

Fig. 5. CD spectra (side-chain region) in ethanol for various values of R. θ is the molar ellipticity.

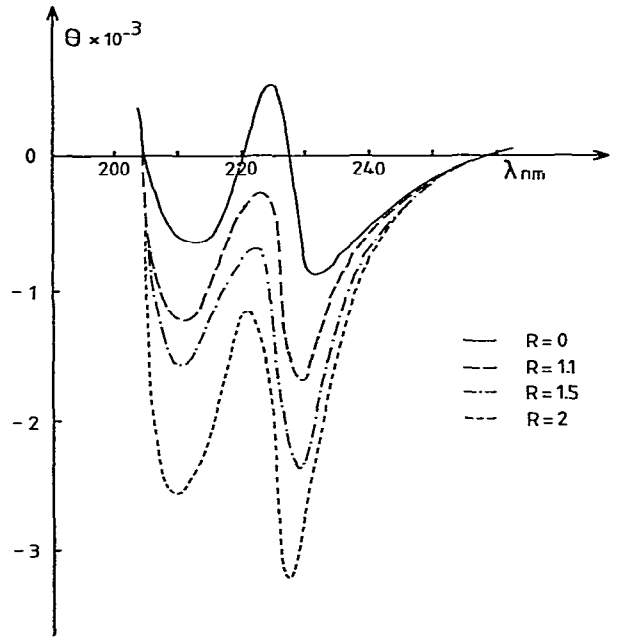

Fig. 6. CD spectra (peptide region) in methanol for various values of R. θ is the residue ellipticity.

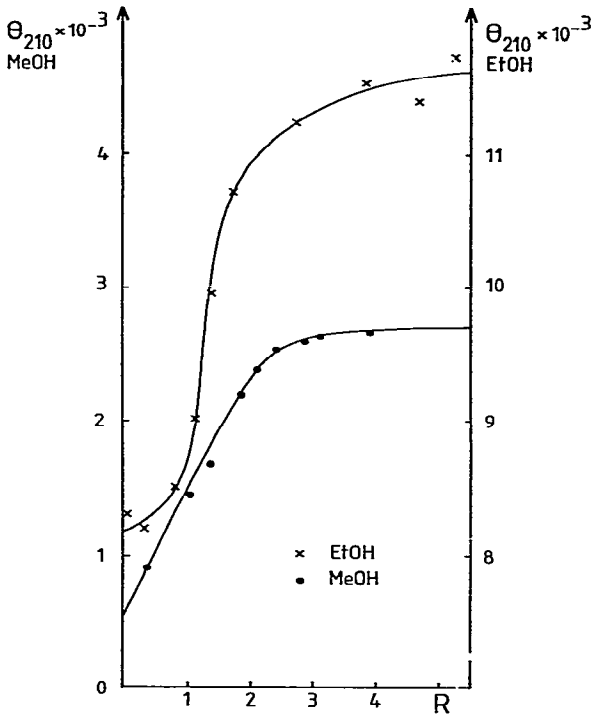

Fig. 7. Variations of the residue ellipticity at 210 nm versus R in methanol and ethanol.

(fig. 3). However, further addition of calcium does not lead to a spectrum characterized by a single amide I band centered around 1653 cm^{-1}. From these investigations, it can be concluded that calcium interacts with gramicidin and induces, at least, partial conformational modifications of this molecule. It must also be mentioned that addition of $ZnCl_2$ (Zn^{2+} does not block the channel) instead of $CaCl_2$ does not induce any modification of the infrared spectrum, indicating clearly that the observed effect can be attributed to Ca^{2+}.

3.1.2. Circular dichroism

The fact that calcium interacts with gramicidin is confirmed by a CD study. Indeed, additions of $CaCl_2$ to solutions of gramicidin in methanol or ethanol induce modifications of the CD spectra, both in the peptide region (200–220 nm) (figs. 4 and 6) and in the tryptophanyl side-chain region (fig. 5). More interestingly, these modifications occur mainly when R is varied from 0 up to around 2 (this appears clearly in fig. 7 for the study in methanol) while further additions do not, or nearly not, modify the spectra. These results suggest that a gramidicin A molecule has two calcium-binding sites.

3.1.3. ^{13}C-NMR spectroscopy

For increasing values of R up to 2, ^{13}C-NMR spectroscopy at 22.63 MHz of a solution of gramicidin in methanol reveals important modifications in the carbonyl resonance spectrum (Fig. 8) while no changes occur on further addition of calcium confirming, thus, the infrared and CD investigations. Moreover, as revealed by spectrum b in fig. 8 obtained for $R = 1$, the first calcium-binding site is close to the formyl group.

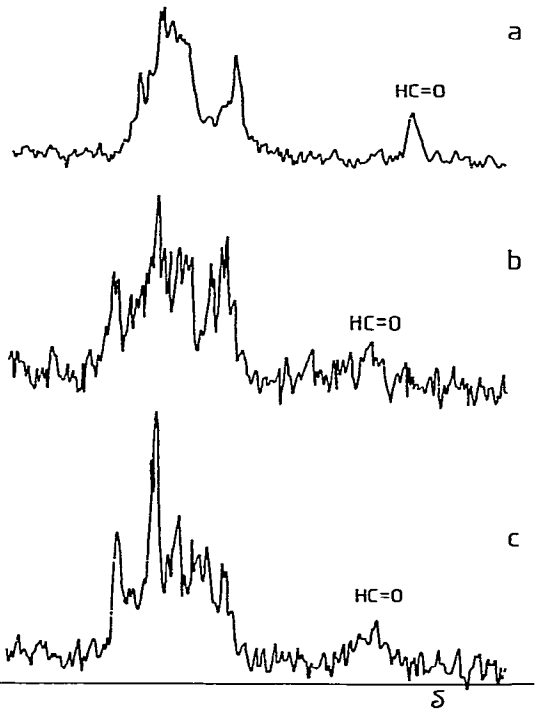

Fig. 8. ^{13}C-NMR spectra (carbonyl region) in C^2H_3OH for increasing values of R. (a) $R = 0$, (b) $R = 1$, (c) $R = 2$.

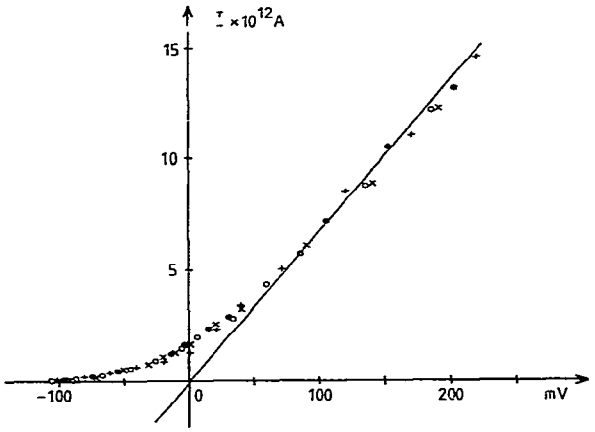

Fig. 9. Single-channel current as a function of the potential difference between the two aqueous sides of glyceryl monooleate/decane membranes. Aqueous solutions were CsCl (1 M) in one side and $CaCl_2$ [concentrations (○) 0.125 M; (×) 0.25 M; (●) 0.5 M and (+) 1 M] in the other. The positive current corresponds to a flow of positive electrical charge from the CsCl side to the $CaCl_2$ one. Corrections due to the difference in electrode potential were made. The full line represents the single-channel current obtained with pure CsCl (1 M) on both sides.

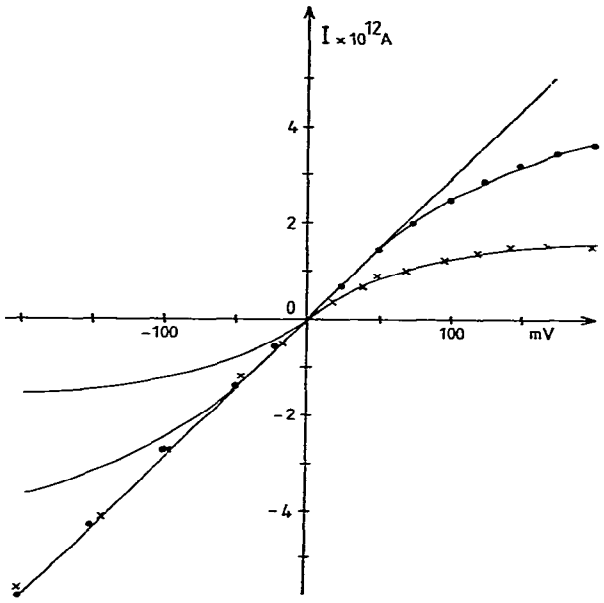

Fig. 10. Variations of the single-channel current as a function of the potential difference between the two aqueous sides. Full lines correspond to symmetrical systems: (●) 0.25 M CsCl on one side and 0.25 M CsCl + 0.5 M $CaCl_2$ on the other, and (×) 0.25 M CsCl on one side and 0.25 M CsCl + 1 M $CaCl_2$ on the other.

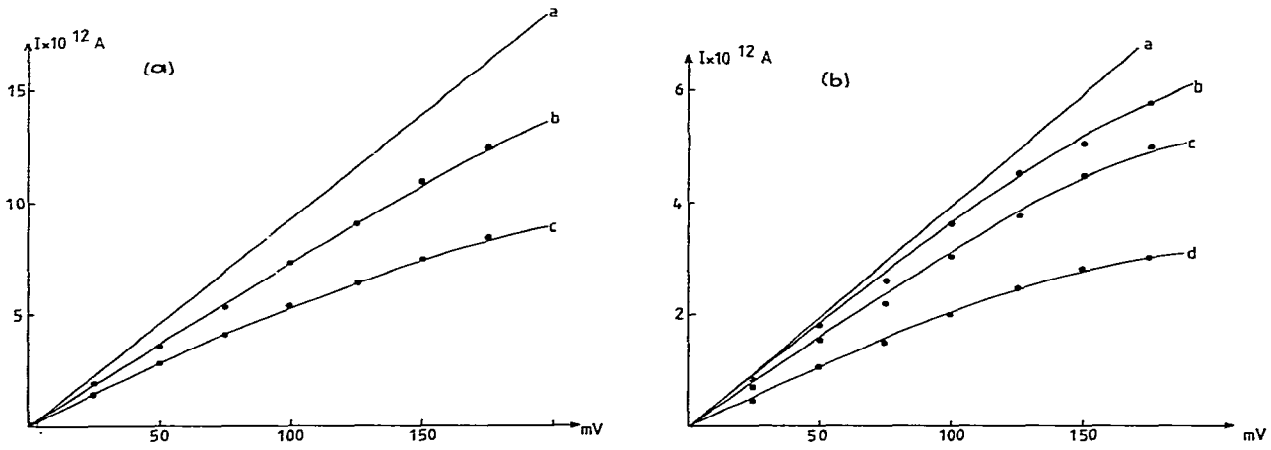

Fig. 11. (a) Variations of the single-channel current in 3 M CsCl containing (1) 0 M $CaCl_2$, (b) 0.5 M $CaCl_2$, (c) 1 M $CaCl_2$. (b) Variations of the single-channel current in 1 M KCl, containing (a) 0 M $CaCl_2$, (b) 0.25 M $CaCl_2$, (c) 0.5 M $CaCl_2$ and (d) 1 M $CaCl_2$.

3.2. Single-channel conductances

Fig. 9 shows the variation of the gramicidin single-channel current versus the potential difference between the two aqueous sides. One aqueous side contains only $CaCl_2$ at various concentrations while the other contains only 1 M CsCl. The current fluctuations always indicate that only Cs^+ crosses the gramicidin channel. The same figure also shows that at high applied voltages the current is the same as that obtained for the 1 M CsCl symmetrical system. The same holds true for other concentrations of CsCl (0.5 and 0.25 M). Such a behavior confirms that the gramicidin A channel is not permeable to Ca^{2+} and shows that, under these conditions, Ca^{2+} does not influence the transfer of Cs^+.

The same conclusion can be drawn from the results shown in fig. 10. Indeed, this figure shows the single-channel current obtained for dissymmetrical aqueous phases. They are symmetrical in their Cs^+ content, the dissymmetry being due to the addition of $CaCl_2$ only in one compartment of the cell. When the current direction corresponds to a Cs^+ transfer from the Ca^{2+}-containing side to the Ca^{2+}-free side, the single-channel current is the same as that obtained for a symmetrical Ca^{2+}-containing system, while it behaves identically to a symmetrical Ca^{2+}-free system when Cs^+ flows in the opposite direction. It must also be mentioned that the behavior in Ca^{2+}-containing symmetrical systems is in full agreement with that already described by Bamberg and Läuger [10]. A similar Ca^{2+}-induced blocking effect is observed on a 3 M CsCl solution and when the alkali metal ion is K^+ (fig. 11a and b).

4. Discussion

From spectroscopic investigations, it can be concluded that calcium interacts with gramicidin A and that one gramicidin molecule has two calcium-binding sites, one of them being located close to the formyl moiety.

The existence of two calcium-binding sites per gramicidin molecule, i.e., four sites on the basis of a dimer, is apparently in opposition with the observations made by Urry et al. [11]. However, it must be remembered that in the present work, measurements have been made on bulk alcoholic solutions while the work described by Urry et al. was made on gramicidin-containing vesicles. In that case, the binding site close to the formyl moiety is not accessible to Ca^{2+}. Indeed, as shown by Weinstein et al. [13], the COOH terminus of gramicidin is located near the surface of the membrane while the NH_2 terminus, and therefore the formyl group, is buried deep within the lipid bilayer, favoring thus the head-to-head dimer model. Therefore, it can be stated that in a lipid bilayer membrane, a gramicidin channel formed by a head-to-head dimer has two calcium-binding sites which are only accessible from the adjoining aqueous solutions and, thus, probably located near the COOH termini. Further, as no transmembrane current can be detected when the electrolyte contains only Ca^{2+}, the translocation of Ca^{2+} between the two binding sites cannot take place. This was explained by Urry et al. [11] on the basis of an estimation of the height of the central energy barrier for divalent cations which could be greater than 20 kcal/mol due to the charge-squared dependence.

As to the Ca^{2+} effect on the single-channel current, let us first discuss the influence on the transfer of Cs^+ at low Cs^+ concentrations. As when the electrical potential is negative in the Ca^{2+}-containing aqueous side the channel current arising from Cs^+ crossing the channel is the same as that obtained without calcium (see figs. 9 and 10) and as a nonlinear I-V response is generated by the addition of Ca^{2+} to the Cs^+ entry side, it can be assumed that the binding of Ca^{2+} from the aqueous phase to its binding site is a voltage-dependent process. Further, owing to the large electrostatic repulsions occurring in the channel due to the double elementary charges of Ca^{2+} it can be assumed that the binding of Ca^{2+} in the channel is competitive with that of Cs^+. Finally, as in this first case where the Cs^+ concentration does not exceed 1 M, the model can be restricted to that which contains at most two monovalent ions in the channel [14]. On this basis, all possible occupancy states are represented in fig. 12 where X designates a site occupied by a Cs^+, Y a site occupied by a

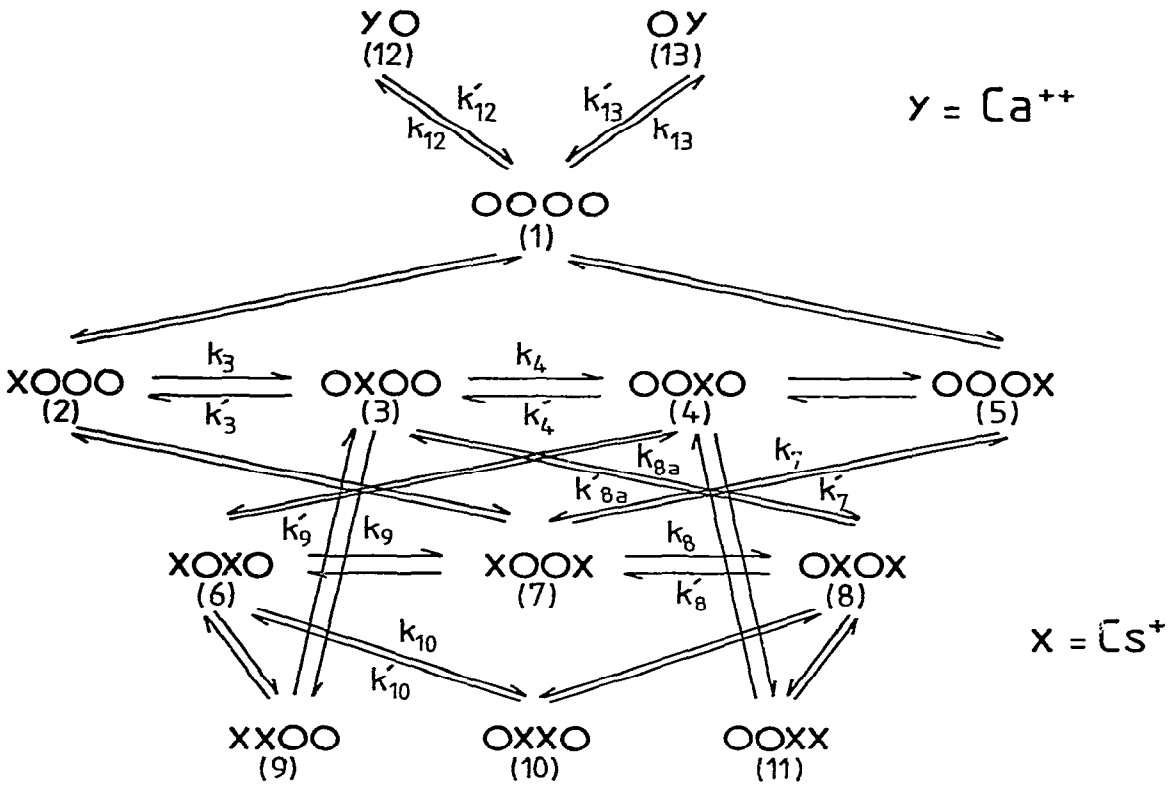

Fig. 12. Scheme of the various situations of site occupancies.

Ca^{2+} and O an empty site; the arrows indicate the possible transitions between two states. Actually, for low CsCl concentrations (0.25 M), the scheme of fig. 12 will be limited to the states 12, 13 and 1–5.

In order to define the single-channel current, the general treatment proposed by Sandblom et al. [15] and used by Urry et al. [16] will be applied to the model proposed here.

The probabilities P_1, $P_2 \ldots P_{13}$ of each state of the scheme of fig. 12 at the steady state for the transfer of monovalent ions can be obtained from a set of 11 equations. P_2 and P_5 can be expressed on the basis of the '3B4S' model already proposed by Sandblom et al. [17]. In this model, the transfer of monovalent cations from the aqueous phase to the outer site is not carried out through an energy barrier. Therefore, the probabilities of occupancy of the outer sites (P_2 and P_5) are related to the probability of state 1 (zero occupancy) and to the ionic activity of Cs^+ through very simple relations:

$$P_2 = K_1 a'_1 P_1 \tag{1}$$

and

$$P_5 = K_1 a''_1 P_1 \tag{2}$$

where a'_1 and a''_1 are the ionic activities of Cs^+ in compartment ′ and ″, respectively.

For the other states, the probabilities are obtained from the set of kinetic equations, eqs. 3–11, at the steady state

$$\frac{dP_3}{dt} = 0 = k_3 P_2 + k'_4 P_4 + k'_{8a} P_8 + k'_9 P_9 - P_3(k'_3 + k_{8a} + k_9) \tag{3}$$

and so on up to eq. 11 for dP_4/dt to dP_{11}/dt where the rate constants k_i are functions of the potential difference between the two aqueous sides. Concerning Ca^{2+}, as its binding, in the model discussed here, is assumed to be potential dependent, the rate constants will depend on the potential difference between the two sides of the membrane ($V' - V''$)

$$k_i = k_i^{\circ} \exp(\alpha_i U)$$

with

$$U = \frac{F(V' - V'')}{RT}$$

where k_i° is the standard rate constant and α_i the coefficient of voltage dependence.

Thus, at the steady state

$$\frac{dP_{12}}{dt} = 0 = a_2' k_{12}^{\circ} P_1 \exp(2\alpha_{12} U) - k''^{\circ}_{12} P_{12} \exp(-2\alpha_{12}' U)$$

and

$$\frac{dP_{13}}{dt} = 0 = a_2'' k_{13}^{\circ} P_1 (-2\alpha_{12} U) - k''^{\circ}_{13} P_{13} \exp(2\alpha_{12}' U)$$

as $k_{13}^{\circ} = k_{12}^{\circ}$ and $k''^{\circ}_{13} = k''^{\circ}_{12}$; the probabilities of states 12 and 13 are

$$P_{12} = K_{Ca} a_2' P_1 \exp(2\alpha_{Ca} U) \qquad (12)$$

and

$$P_{13} = K_{Ca} a_2'' P_1 \exp(-2\alpha_{Ca} U) \qquad (13)$$

with $K_{Ca} = k_{12}^{\circ}/k''^{\circ}_{12}$, $\alpha_{Ca} = \alpha_{12} + \alpha_{12}'$ and a_2' and a_2'' the activities in compartment ' and '', respectively. From these equations, the single-channel current at the steady state then follows (see appendix A)

$$I = \frac{vFP_1^{\circ}}{1 + P_1^{\circ} K_{Ca} [a_2' \exp(2\alpha_{Ca} U) + a_2'' \exp(-2\alpha_{Ca} U)]} \qquad (14)$$

where v is a function of U, a_1', a_1'' and of the standard rate constants. From eq. 14, it appears that when there is no Ca^{2+} in the Cs^+-containing compartment the single-channel current obtained at high voltages has the same value as that obtained with a totally calcium-free system (see fig. 9).

For a symmetrical calcium concentration ($a_2' = a_2'' = a_2$), for a given cesium concentration and a given voltage, the ratio I_0/I of the single-channel currents without and with calcium is given by:

$$I_0/I = 1 + 2P_1^{\circ} K_{12} a_2 \cosh(2\alpha_{Ca} U) \qquad (15)$$

which leads to the ratio of limiting conductances

$$\frac{\lambda_{00}}{\lambda_0} = 1 + 2P_1^{\circ} K_{12} a_2 \qquad (16)$$

On the basis of the results obtained by Bamberg and Läuger [10], we have reported in fig. 13 the variation of the ratio λ_{00}/λ_0 with the concentration of Ca^{2+}. This figure shows that eq. 16 accounts quite satisfactorily for the experimental values obtained using Ca^{2+} (curves a and b) but also for Ba^{2+} (curve c). This figure also reveals that the variations of the ratio λ_{00}/λ_0 depend on the nature of the bilayer-forming lipid. This result suggests that the equilibrium constant for the binding of Ca^{2+} to its gramicidin site also depends on the nature of the surrounding lipids, as already observed for alkali metal ions [10].

In order to test the validity of eq. 15, in fig. 14 we have plotted $I_0/I - 1$ as a function of the reduced voltage U (experimental points). This figure shows that, up to 125 mV, the variation of I_0/I follows eq. 15 (full lines) where the values of $\alpha_{Ca^{2+}}$ have been chosen to obtain the best fit, indicating clearly that the blocking effect of calcium is voltage dependent. Therefore, from these results, the voltage dependence coefficient $\alpha_{Ca^{2+}}$ which reflects the electrical distance of the binding site inside the channel can be determined. Its value is 0.145 in diphytanoylphosphatidylcholine on the basis of the work of Bamberg and Läuger [10] and 0.165 in glyceryl monooleate. It must be mentioned here that for glyceryl monooleate bilayers, within the alkali metal cation family, this coefficient increases steadily when the ionic radius decreases (from 0.18 for Cs^+ to 0.38 for Li^+ [18]). Using another representation, the variation of $I_0/I - 1$ with $\cosh 2\alpha U$ at low potentials shows a linear behavior which for $U = 0$, can be extrapolated to the value $I_0/I - 1 = 0$, corroborating thus the above conclusion (fig. 15).

When the concentration of Cs^+ is increased up to 3 M, the general trend is the same as that discussed above. Indeed, the $(I_0/I - 1)$ vs. $(\cosh 2\alpha U)$ plots, using the same values of α as previously, also show a linear behavior indicating again a Ca^{2+}-induced voltage-dependent blocking effect. However, the extrapolation at zero voltage also reveals a concentration effect of Ca^{2+} (fig.

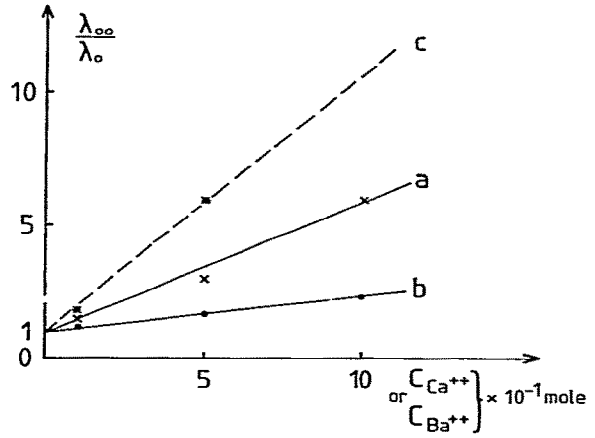

Fig. 13. Variations of the ratio of the limiting conductances $\lambda_{\infty}/\lambda_0$ versus the Ca^{2+} concentration. (a) Diphytanoylphosphatidylcholine membrane in 1 M CsCl (from ref. 10). (b) As curve a as but glyceryl monooleate membrane [10]. (c) Dioleoylphosphatidylcholine membrane in 1 M CsCl [10]. Ba^{2+} instead of Ca^{2+}. Note that as the values of the activity coefficients of Ca^{2+} are unknown for the considered experimental conditions (the electrolyte contains two different cations Cs^+ and Ca^{2+}), we have reported in this figure the variation of $\lambda_{\infty}/\lambda_0$ with the concentration of Ca^{2+} instead of the activity and it must be recalled that in the concentration range 0.1–1 M, the activity coefficient goes through a minimum for pure $CaCl_2$ [19].

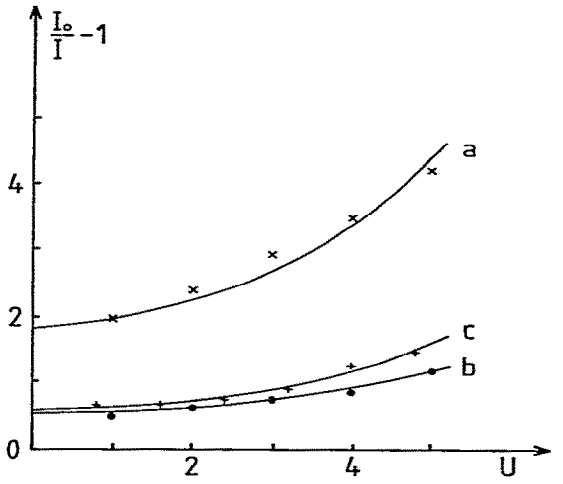

Fig. 14. Variations of $I_0/I-1$ versus U. (X) Diphytanoylphosphatidylcholine membrane, 1 M CsCl + 0.5 M $CaCl_2$ (from ref. 10). Curve a corresponds to the equation: $I_0/I-1 = 1.919\cosh 0.29U$. (●) As for X, but 0.1 M $CaCl_2$ [10]. Curve b: $I_0/I-1 = 0.53\cosh 0.29U$. (+) Glyceryl monooleate membrane. 0.25 M CsCl + 1 M $CaCl_2$. Curve c: $I_0/I-1 = 0.60\cosh 0.33U$.

15). To account for this result, it is necessary to improve the model shown in fig. 12 by addition of two supplementary binding sites. The binding of Ca^{2+} to these new sites is again competitive with that of Cs^+ but it is voltage independent. These sites are external with respect to the channel and they block only the entry step and not the exist step.

The probabilities for a Ca^{2+} of occupying one of these two sites (P_{i4} and P_{i5}) are again proportional to P_i and to the Ca^{2+} activities in the aqueous media

$$P_{i4} = K_e a'_2 P_i \tag{17}$$

and

$$P_{i5} = K_e a''_2 P_i \tag{18}$$

where K_e is independent of the voltage. Taking into account eqs. 17 and 18 leads to a new expression of the I_0/I ratio

$$I_0/I = 1 + 2P_1^{o} a_2 (K_e + K_{12}\cosh 2\alpha U) \tag{19}$$

The same analysis based on eq. 19 can be applied when the system contains K^+ instead of Cs^+ as shown in fig. 16. Again, the variation of $I_0/I-1$ with $\cosh 2\alpha U$ is linear and depends on the con-

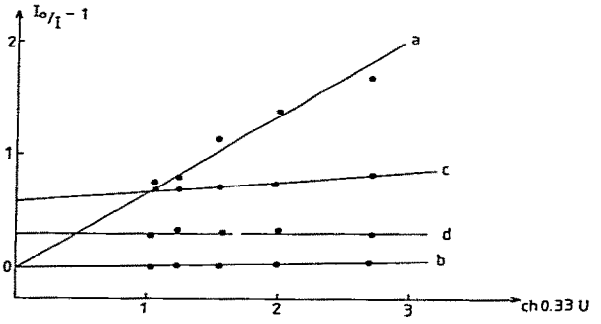

Fig. 15. Variations of $I_0/I-1$ versus $\cosh(0.33U)$. (a) 0.25 M CaCl, 1 M; $CaCl_2$; (b) 0.25 M CsCl, 0.5 M $CaCl_2$; (c) 3 M CsCl, 1 M $CaCl_3$; (d) 3 M CsCl, 0.5 M $CaCl_2$.

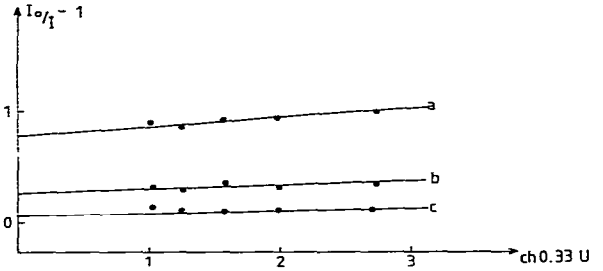

Fig. 16. Variations of $I_0/I-1$ versus cosh(0.33U). (a) 1 M KCl, 1 M $CaCl_2$; (b) 1 M KCl, 0.5 M $CaCl_2$; (c) 1 M KCl, 0.25 M $CaCl_2$.

centration of Ca^{2+}. Thus, on the basis of the initial model and its proposed improvement two limiting situations may exist. In the first one, where only the external sites are occupied, $I_0/I-1$ is independent of the voltage and only depends on $a_{Ca^{2+}}$ while in the second one where only the internal sites are occupied $I_0/I-1$ varies linearly with coshαU and the slopes depend on the Ca^{2+} concentration.

Actually, at 0.25 M CsCl the situation corresponds to the latter situation while under the CsCl 3 M and KCl conditions the situations are intermediate.

The above model is supported by examination of the free energy profiles of the gramicidin A channel already proposed by Eisenman and Sandblom [18]. Indeed, in the case of Cs^+, an increase in the loading state of the channel (from one to two ions) leads to an increase in the free energy of the entry binding site. From the point of view of the experimental results discussed here, this corresponds to the 0.25 M CsCl solution (one ion) and to the 3 M CsCl solution (more than one ion). Therefore, at low Cs^+ concentrations, the entry site is occupied only by the alkali metal ion while Ca^{2+} can compete with Cs^+ at higher Cs^+ concentrations.

Further, the similarity between the behavior observed for the 3 M CsCl solution and that obtained for KCl can be explained by the fact that for K^+ the free energy of the entry binding site is comparable to that of the two-ion state of Cs^+.

In summary, this work shows that the blocking effect of Ca^{2+} on the transfer of alkali metal ions through the gramicidin channel is mainly the result of the binding of Ca^{2+} inside the channel. There are two major binding sites per dimer channel and they are located near the COOH termini. The binding of Ca^{2+} is competitive with the uptake of Cs^+ and for these major binding sites it is voltage dependent, the voltage dependence coefficient being around 0.15.

Appendix A

A1. Derivation of eq. 14

The sum of the probabilities of all the states is unity

$$\sum_{i=1}^{i=11} P_i = 1 \tag{A1}$$

The system of the linear equations from eq. 1 to eq. 11 can be solved and therefore, each probability can be obtained as a function of P_1

$$P_2 = \lambda_2 P_1 \tag{A2}$$

$$P_3 = \lambda_3 P_1 \tag{A3}$$

$$\vdots$$

$$P_{11} = \lambda_{11} P_1 \tag{A11}$$

$\lambda_2 \ldots \lambda_{11}$ are functions of the standard rate constants k_i^o, $k_i'^o$, of the reduced voltage U and of the ionic activities a_1' and a_2'. In the absence of Ca^{2+}, P_1 is termed P_1^o and combining eq. A1 with eqs. A2–A11 leads to

$$P_1^o = \frac{1}{1+\sum_{i=2}^{i=11} \lambda_i} \tag{A12}$$

When Ca^{2+} is present in the aqueous media, the preceding equation gives

$$P_1 = P_1^o[1-(P_{12}+P_{13})] \tag{A13}$$

Combination of eq. A13 with eqs. 12 and 13 leads to

$$P_1 = \frac{P_1^o}{1+P_1^o K_{Ca}[a_2' \exp(2\alpha_{Ca}U)+a_2'' \exp(-2\alpha_{Ca}U)]} \tag{A14}$$

As Ca^{2+} does not cross the channel, at the steady state, the current depends only on the flux

charges carried by Cs^+. The flux of Cs^+ crossing the channel can be calculated considering the number of Cs^+ transferred between to adjoining Cs^+-binding sites in the channel, for instance, the first and the second sites

$$I = F(k_3 P_2 - k_3' P_3 + k_8 P_7 - k_8' P_8 + k_{10} P_6 - k_{10}' P_{10}) \quad \text{(A15)}$$

Eqs. A15, A14 and A2–A11 lead to

$$I = \frac{\upsilon F P_1^\circ}{1 + P_1^\circ K_{Ca}[a_2' \exp(2\alpha_{Ca} U) + a_2'' \exp(-2\alpha_{Ca} U)]}$$

with

$$\upsilon = k_3\lambda_2 - k_3'\lambda_3 + k_8\lambda_7 + k_8'\lambda_8 + k_{10}\lambda_6 - k_{10}'\lambda_{10}$$

Acknowledgements

The authors are grateful to Dr. G. Spach for helpful discussions and continuous interest in this work. This work was supported by grant RCP 80-605 from C.N.R.S.

References

1 R. Sarges and B. Witkop, J. Am. Chem. Soc. 87 (1965) 2011.
2 D.W. Urry, Proc. Natl. Acad. Sci. U.S.A. 69 (1972) 1610.
3 J.D. Glickson, D.F. Mayers, J.M. Settine and D.W. Urry, Biochemistry 11 (1972) 477.
4 D.A. Haydon and S.B. Hladky, Q. Rev. Biophys. 5 (1972) 187.
5 S.B. Hladky and D.A. Haydon, Biochim. Biophys. Acta 274 (1972) 294.
6 E. Bamberg, K. Noda, E. Gross and P. Läuger, Biochim. Biophys. Acta 419 (1976) 223.
7 V.B. Myers and D.A. Haydon, Biochim. Biophys. Acta 274 (1972) 313.
8 D. Busath and G. Szabo, Nature 294 (1981) 371.
9 F. Heitz, G. Spach and Y. Trudelle, Biophys. J. 39 (1982) 87.
10 E. Bamberg and P. Läuger, J. Membrane Biol. 35 (1977) 351.
11 D.W. Urry, J.T. Walker and T.L. Trapane, J. Membrane Biol. 69 (1982) 225.
12 G. Eisenman, J. Sandblom and J. Hagglund, in: Structure and function of excitable membranes, eds. W. Adelman, D. Chang, R. Leuchtag and I. Tasoki (Plenum Press, New York, 1983) in the press.
13 S. Weinstein, B.A. Wallace, E.R. Blout, J.S. Morrow and W. Veatch, Proc. Natl. Acad. Sci. U.S.A. 76 (1979) 4230.
14 G. Eisenman, J. Hagglund, J. Sandblom and B. Enos, Uppsala, J. Med. Sci. 85 (1980) 247.
15 J. Sandblom, G. Eisenman and E. Neher, J. Membrane Biol. 31 (1977) 383.
16 D.W. Urry, G.M. Ventakachalam, A. Spini, P. Läuger and M. Abukaled, Proc. Natl. Acad. Sci. U.S.A. 77 (1980) 2028.
17 J. Sandblom, G. Eisenman and J. Hagglund, J. Membrane Biol. 71 (1983) 61.
18 G. Eisenman and J. Sandblom, in: Physico-chemistry of ion movement in membranes, ed. G. Spach (Elsevier, Amsterdam, 1983) in the press.
19 R.A. Robinson and R.H. Stokes, Electrolyte solutions (Butterworths, London, 1952) p. 482.